

## A spaceborne neodymium-doped yttrium aluminum garnet laser with nonplanar-ring-oscillator configuration

Jiankang Peng<sup>\*,†</sup>, Liufeng Li<sup>\*,‡,§,¶</sup> and Lisheng Chen<sup>\*,†,‡,§,¶</sup>

<sup>\*</sup>Innovation Academy for Precision Measurement Science and Technology,  
Chinese Academy of Sciences, Wuhan 430071, China

<sup>†</sup>University of Chinese Academy of Sciences, Beijing 100049, China

<sup>‡</sup>State Key Laboratory of Magnetic Resonance and Atomic  
and Molecular Physics, Wuhan 430071, China

<sup>§</sup>Laboratory of Atomic Frequency Standards,  
Chinese Academy of Sciences, Wuhan 430071, China

<sup>¶</sup>liufengli@apm.ac.cn  
lchen@wipm.ac.cn

Received 15 September 2020

Accepted 30 October 2020

Published 22 March 2021

*\*\*On behalf of The Taiji Scientific Collaboration*

Due to their excellent noise performance and technical maturity, ultra-stable continuous-wave neodymium-doped yttrium aluminum garnet lasers are one of the major light sources in a series of precision measurements such as ground- and space-based gravitational wave detection, inter-satellite laser ranging and coherent optical communication. As the first step of developing an ultra-stable spaceborne laser, we carried out the design, development and environmental test of an all-solid-state Nd:YAG NPRO spaceborne laser. The laser delivers 11.48 mW of optical power at 1064.405 nm, exhibits intensity and frequency noises less than  $1 \times 10^{-2}/\sqrt{\text{Hz}}$  and  $1 \text{ MHz}/\sqrt{\text{Hz}}$  (Fourier frequencies  $> 10 \text{ mHz}$ ), respectively, passed environmental tests and has been onboard the first satellite of the Taiji program for one year. The work laid a solid foundation for realizing ultra-stable lasers for the Taiji program as well as being used in many space applications.

*Keywords:* Nd:YAG; NPRO; gravitational wave detection; spaceborne laser.

### 1. Introduction

In 2015, a century after the prediction<sup>1</sup> of Einstein's theory of general relativity, the laser interferometer gravitational-wave observatory (LIGO) directly detected the gravitational waves (GWs) produced by two merging black holes,<sup>2,3</sup> opening a new window to the universe otherwise can only be perceived by the electromagnetic waves. The ground- and spaced-based GW observatories, linked with a variety of instruments, enable new ways to

<sup>¶</sup>Corresponding authors.

**\*\***For more details, please refer to article 2102002 of this Special Issue.

understand the evolution of the universe, examine basic laws of physics and explore relativistic astrophysical dynamics.

To observe GW in the spectral range from millihertz to hertz, a long-baseline laser interferometer in space was envisaged.<sup>4,5</sup> Lasers with ultra-low frequency and intensity noises are prerequisites for constructing this large-scale and unequal-arm-length Michelson interferometer in which laser ranging and inertial sensing with ultra-high sensitivities are employed.

The Taiji program, proposed by CAS, is one of the Chinese projects for GW detection in space. Its ultimate goal is to detect the GW by using the laser interferometer with million-kilometer arm length and formed by a triangle-shaped constellation of three spacecrafts orbiting the Sun.<sup>6</sup>

As the first step of the program, the Taiji-1 satellite was launched as a technological testing platform, which includes a laser interferometer, an accelerometer, two micro-Newton thrusters and supporting hardware and software. The spaceborne laser onboard the satellite is an independent payload providing a light source for the laser interferometer.

Nd:YAG lasers based on monolithic nonplanar ring oscillators (NPROs)<sup>7,8</sup> of different variants are the workhorse of the GW detection on the ground as well as in space that will be realized in the foreseeable future. The monolithic NPRO laser was first proposed and developed by Kane, Byer and Zhou of Stanford University in the mid-1980s. Exhibiting a low frequency noise, with high beam quality and being compact and lightweight, the laser has been successfully used in many space missions such as LISA pathfinder.<sup>9</sup> Here, the Nd:YAG NPRO laser is again chosen as the light source for the laser interferometer onboard the Taiji-1 satellite.

The design of the first satellite of the Taiji program demands a continuous wave (CW) laser with an output power of  $(10 \pm 3)$  mW and a wavelength of  $(1064.5 \pm 1.0)$  nm. In addition, the frequency and the intensity noises should be controlled, respectively, below  $1 \text{ MHz}/\sqrt{\text{Hz}}$  and  $1 \times 10^{-2}/\sqrt{\text{Hz}}$  at Fourier frequencies above 10 mHz. Satellite launch and space environment impose strict control of the volume, weight, power consumption, mechanical structure and electromagnetic compatibility (EMC).<sup>10</sup> To meet these requirements, we carried out the design, development and experimental test of a CW Nd:YAG NPRO laser (Laser B), which is one of the two lasers onboard the Taiji-1 satellite.

## **2. The Development of the Spaceborne Laser**

Figure 1 shows the functional block diagram of the space-borne laser. The monolithic Nd:YAG NPRO is pumped by a diode laser (LD), producing laser radiation at a nominal wavelength of 1064 nm. The pump laser delivers Watt-level light at 808 nm and is driven by a highly stable current source. The temperatures of the pump laser and the monolithic NPRO are actively stabilized to minimize the wavelength fluctuations of both the pump and the NPRO crystal. The laser can be divided into two parts; The monolithic

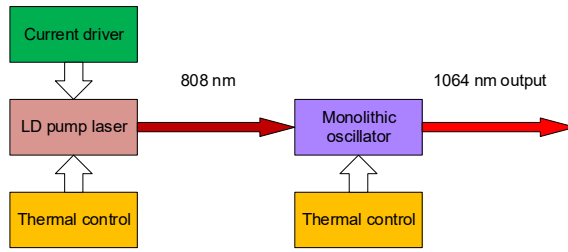


Fig. 1. The block diagram of the spaceborne Nd:YAG NPRO laser.

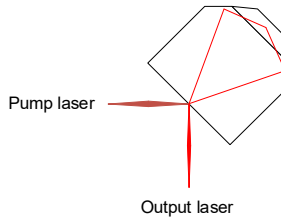


Fig. 2. The optical path of a monolithic NPRO.

NPRO, its auxiliaries and the pump laser form the laser head and the electronic module consists of a secondary power supply, a current driver and a two-channel temperature controller.

Figure 2 illustrates the optical path inside a monolithic NPRO. Lasing is obtained when the loop formed by a round-trip traveling wave is closed. The operation of single longitudinal mode is achieved by introducing a magnetic field to break the symmetry of the two polarization eigenmodes that counter propagate inside the NPRO and hence extinguishing the mode with higher intra-cavity loss.<sup>11,12</sup>

Figure 3 is a structural illustration of the laser head. By optimizing the geometry<sup>13</sup> and the optical coating of the NPRO,<sup>14</sup> reliable unidirectional operation with a reduced magnetic field was realized and the output power is also maximized (see Refs. 15–19 for details). After exiting the NPRO, the 1064-nm light hits upon a mini-size Faraday optical isolator to avoid lasing instability due to the interference between the forward light and the back reflection.

The coupling of the laser into the optical fiber is achieved by fixing an aspheric lens and the ferrule of optical fiber connector on a spherical adjustment structure. The moveable parts on the structure are fine-tuned to optimize the coupling efficiency and then fixed after the optical alignment. This coupling mechanism not only has the feasibility for optical alignment but also maintains structural robustness to withstand mechanical vibration and impact.

A permanent magnet is on top of the monolithic NPRO crystal with a fluor rubber O-ring inserted in between to serve as a buffer. The bottom of the crystal is cemented to a

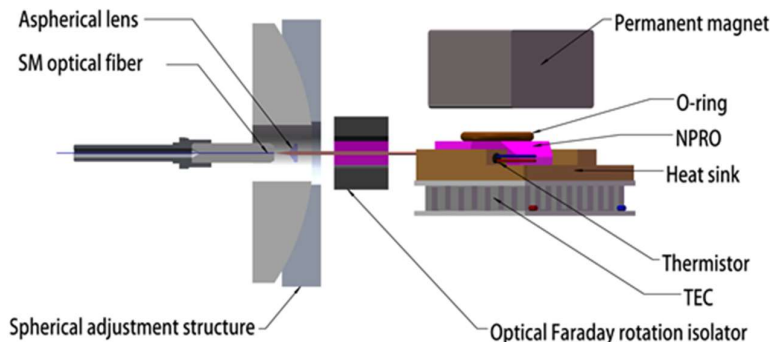


Fig. 3. The assembly of the laser head.

copper heat sink on which position-limiting grooves for the crystal are machined. For temperature stabilization of the NPRO, a thermoelectric cooler (TEC) is installed underneath the heat sink and a thermistor is embedded in the copper heat sink. The NPRO assembly, together with coupling components, is placed inside an airtight metal enclosure.

The electronic module consists of a current driver (current source), a two-channel temperature controller and a secondary power supply that converts the main power supply of the satellite to multiple voltages used by the laser electronics. High-power components are attached to the bottom plate of the enclosure to allow for reliable heat dissipation.

Figure 4 shows the overall appearance of the spaceborne laser, which weighs 3.677 kg and has dimensions of 240 mm × 208 mm × 70 mm.

The NPRO has to be immersed in an atmospheric environment for reliable long-term operation.<sup>20</sup> To accommodate this requirement, the interior of the laser is divided into two cabins. The laser head assembly and the pump LD are inside a one-atmosphere sealed cabin while the electronics are in the second cabin which is connected with the outside. The two cabins are electrically connected via a multi-pin vacuum-compatible feedthrough.

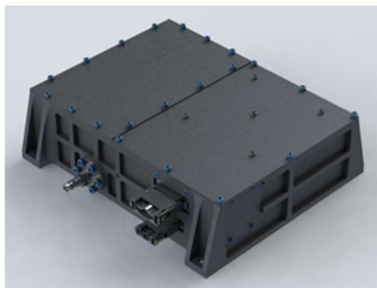


Fig. 4. The CAD rendering of the external view of the spaceborne laser.

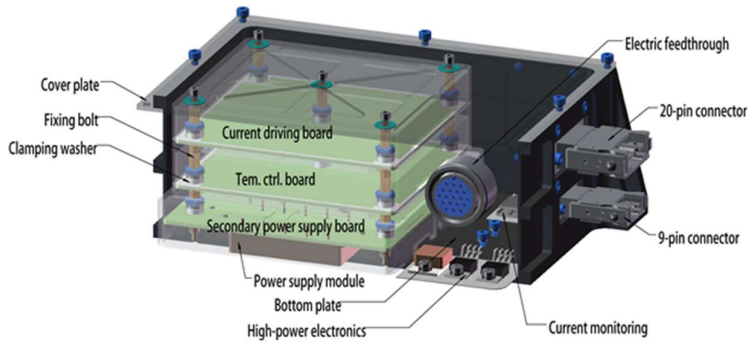


Fig. 5. The CAD rendering of the internal structure of the spaceborne laser.

Finite element analysis (FEA) shows that the stress of the sealed cabin is mainly concentrated in the center of the cabin cover and on the periphery of the set screws, where the maximum stress is  $2.1 \times 10^8 \text{ N/m}^2$ , which is less than the maximum material yield force of  $3.2 \times 10^8 \text{ N/m}^2$ . In addition, tests with pressurized cabin confirmed the structural integrity of the sealed cabin.

Figure 5 shows the mounting strategy of the circuit boards. Here, we adopt a stacked multi-layer structure to facilitate structural reinforcement and heat dissipation while keeping small volume. Added between the circuit boards are electromagnetic shielding enclosures, which press against a large portion of the perimeters of circuit boards, restricting the membrane-vibration modes of the circuit board during impact and adding additional dissipation path for heat generated on the circuit board.

### 3. Environment and Performance Tests

Environment tests were performed on the key components and the laser unit. Mechanical tests were sinusoidal vibrations (3.3–5.3 g,  $X$ ,  $Y$  and  $Z$ ), random vibrations (8.1–10.2 g,  $X$ ,  $Y$  and  $Z$ ), and shock test in which the peak acceleration during the impact reached 800 g ( $X$ ,  $Y$  and  $Z$ ). Totally 426 h were accumulated in the thermal cycling and the vacuum test, including a 76-h screening of the circuit boards. The laser also passed an EMC test.

The output power of the laser is 11.48 mW, and the wavelength is 1064.405 nm when tested on the ground. Figure 6 shows the intensity and frequency noises of the laser at Fourier frequencies of 5 mHz–0.5 Hz. To measure the laser frequency noise, a cavity-stabilized Nd:YAG laser operating in the laboratory was used as a frequency reference. The laser under test was beat against the reference laser to obtain the frequency noise. Above 10 mHz, the laser frequency and intensity noises are less than  $1 \text{ MHz}/\sqrt{\text{Hz}}$  and  $1 \times 10^{-2}/\sqrt{\text{Hz}}$ , respectively.

The function and performance of the laser were tested after the satellite was in its orbit. The temperatures at various monitoring locations, including the installation plate, the surface of the laser, the pump LD and the NPRO, are all within the range of the

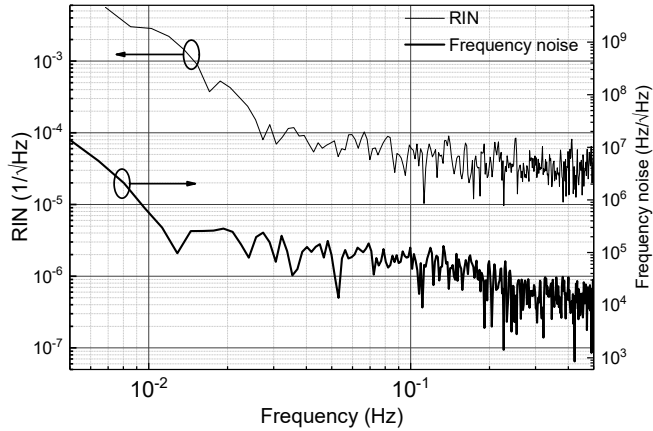


Fig. 6. Intensity and frequency noises of the spaceborne laser measured at 1064.405 nm.

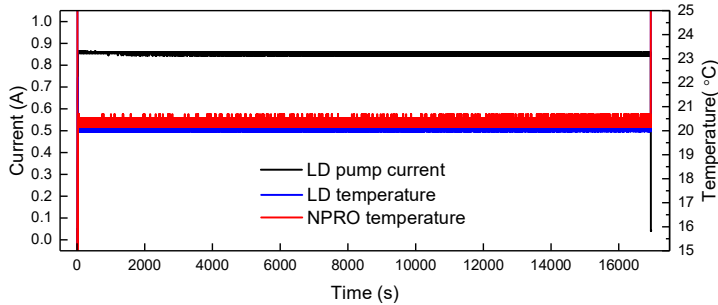


Fig. 7. Monitoring signals of the laser on board the satellite. The jumps at the beginning and the end are transit process during switch on and off.

design specification. The in-orbit monitoring signals agree with the ground test. Figure 7 shows a data of more than 4 h of monitoring signals of the laser.

#### 4. Summary and Outlook

By optimizing the geometry of the resonant cavity and adopting structural reinforcement, a 1064-nm spaceborne laser based on the monolithic Nd:YAG NPRO is developed. The laser output power is 11.48 mW and above 10 mHz the frequency and intensity noises are less than 1 MHz/ $\sqrt{\text{Hz}}$  and  $1 \times 10^{-2}/\sqrt{\text{Hz}}$ , respectively. The laser passed the environmental test and was onboard the Taiji-1 satellite. The monitoring singles verified its functionality after the satellite was launched into orbit.

Our next step is to develop a space-version high-finesse optical cavity for frequency stabilization. The optical power and frequency of the space-borne laser will be actively controlled to meet the noise budget required for space GW detection.

The Nd:YAG NPRO laser developed here realized our first step towards an ultra-stable spaceborne laser that will play an important role in many space applications, including GW detection in space, retrieval of Earth gravitational field using satellite laser ranging, and inter-satellite coherent data link.

## Acknowledgments

We thank Shaofeng An, Qin Wang, Fang Wang, Li Wang at APM, CAS for their assistance in developing and testing phases. We acknowledge the contribution from Zhi Wang and Wei Sha, both at the Changchun Institute of Optics, Fine Mechanics and Physics, CAS, for valuable advice on the optical design and adjustment; Suggestions from Jianjun Jia at Shanghai Institute of Technical Physics, CAS are highly appreciated. This work is supported by the Strategic Priority Research Program of the Chinese Academy of Sciences (Grant Nos. XDA15020703, XDB21010300 and XDB23030202), National Key RD Program of China (2017YFA0304403) and the National Natural Science Foundation of China (Grant No. 11654004).

## References

1. A. Einstein, *Näherungsweise Integration der Feldgleichungen der Gravitation*, Part 1. (Sitzungsberichte der Königlich Preussischen Akademie der Wissenschaften, Berlin, 1916), pp. 688–696.
2. LIGO Scientific and Virgo Collabs. (B. P. Abbott *et al.*), *Phys. Rev. Lett.* **116**, 061102 (2016).
3. LIGO Scientific and Virgo Collabs. (B. P. Abbott *et al.*), *Phys. Rev. Lett.* **116**, 241103 (2016).
4. The LISA Study Team (P. Bender), Laser interferometer space antenna for the detection of gravitational waves, pre-phase a report, Max-Planck-Institute for Quantum Optics, MPQ233 (1998).
5. The LISA Study Team (K. Danzmann), *Adv. Space Res.* **32**, 1233 (2003).
6. W.-R. Hu and Y.-L. Wu, *Natl. Sci. Rev.* **4**, 685 (2017).
7. T. J. Kane, R. L. Byer and B. K. Zhou, Monolithic single-mode Nd:YAG ring laser, in *Conf. Lasers and Electro-Optics*, USA, Digest WM3, 1984, p. 114.
8. T. J. Kane and R. L. Byer, *Opt. Lett.* **10**, 65 (1985).
9. M. Armano *et al.*, *Phys. Rev. Lett.* **116**, 231101 (2016).
10. G. A. Jackson, Setting the standards—the European EMC Directive, *IEE Review*, **36**, 143 (1990).
11. A. C. Nilsson and E. K. Gustafson, *IEEE J. Quantum Electron.* **25**, 767 (1989).
12. E. A. Cheng and T. J. Kane, *Opt. Lett.* **16**, 478 (1991).
13. W. Ke-Ying, Y. Su-Hui, Z. Chang-Ming *et al.*, *Chin. Phys. Lett.* **17**, 728 (2000).
14. A. R. Globes and M. J. Brienza, *Appl. Phys. Lett.* **21**, 265 (1972).
15. E. Zang, H. Cao, K. Zhao *et al.*, Monolithic quasi-planar ring lasers, in *Proc. SPIE* (Shanghai, China, 1998), pp. 29–34.
16. E. J. Zang, J. Cao, M. Zhong *et al.*, *Appl. Opt.* **41**, 7012 (2002).
17. E. Zang, J. Cao, M. Zhong *et al.*, Output power and frequency stability of monolithic semi-nonplanar ring lasers, in *SPIE*, Vol. 4914, (Beijing, China, 2002), pp. 276–279.
18. W. Deng, T. Yang, J. Cao *et al.*, *Opt. Lett.* **43**, 1562 (2018).
19. I. Freitag, A. Tünnermann and H. Welling, *Opt. Commun.* **115**, 511 (1995).
20. X.-L. Ling, Y.-A. Zhao, D.-W. Li *et al.*, *Chin. Phys. Lett.* **26**, 074203 (2009).